

# Towards a Predictive Theory of Polycrystal Coarsening: Experiments and Simulations

**K. Barmak**

Department of Applied Physics and  
Applied Mathematics  
Columbia University





APAM in SEAS at  
Columbia University in  
the City of New York

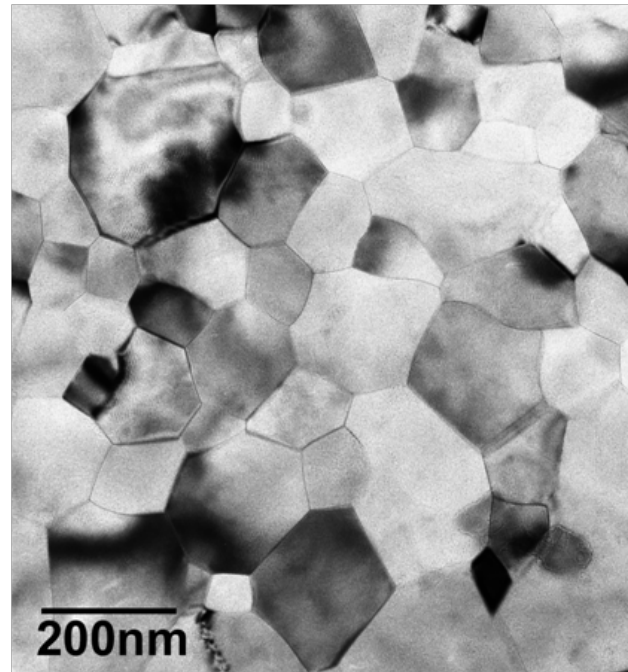
- Applied Physics
- Applied Mathematics
- Materials Science and Engineering
- Medical Physics

# Polycrystals: The Challenge

Development of prescriptive process technologies capable of producing an arrangement of grains that provides for a desired set of materials properties.

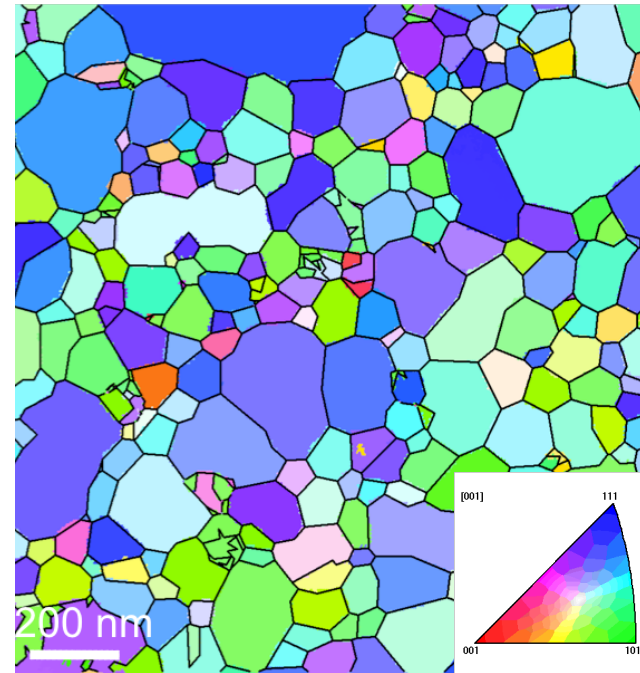
**Aluminum**

Ex-Situ Experiment:  
Bright-field  
transmission electron  
micrograph



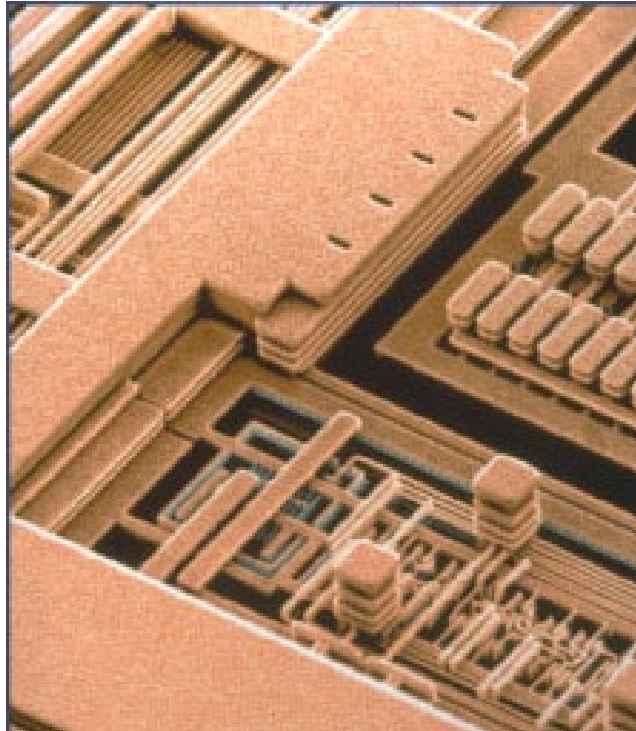
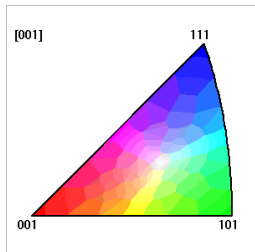
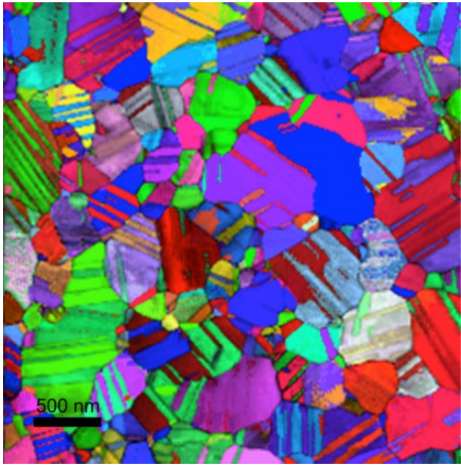
**Aluminum**

Ex-Situ Experiment:  
Precession electron  
diffraction crystal  
orientation map of  
annealed sample

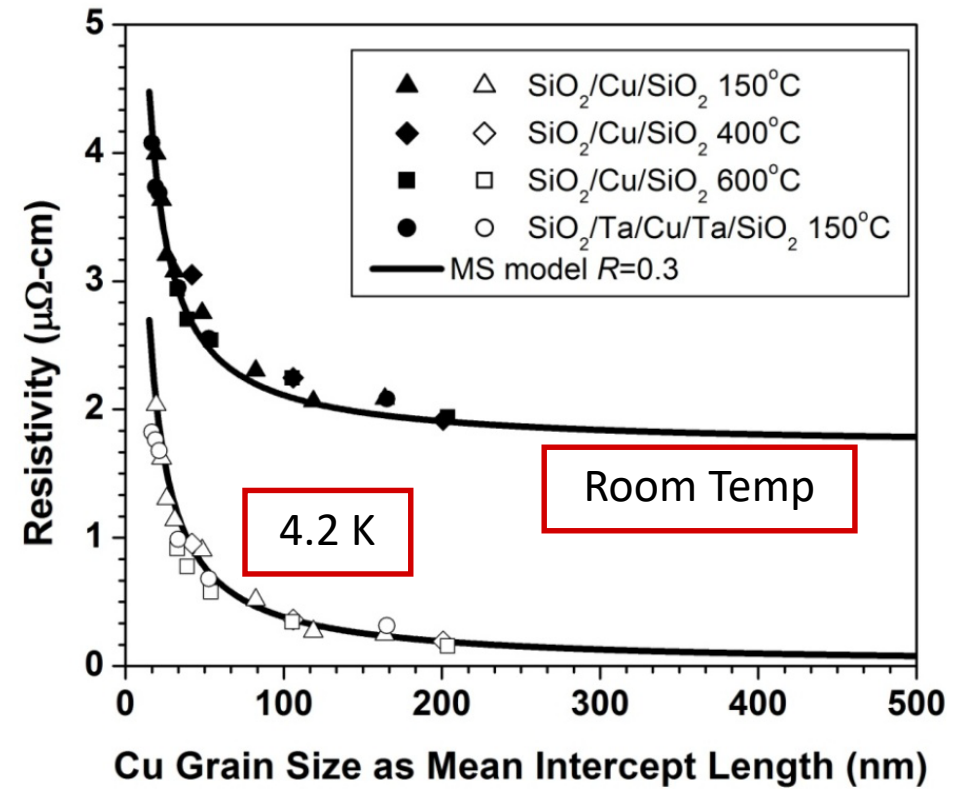




# Impact of Structure on Property



IBM CMOS 7S  
ASIC with 6 levels of Cu

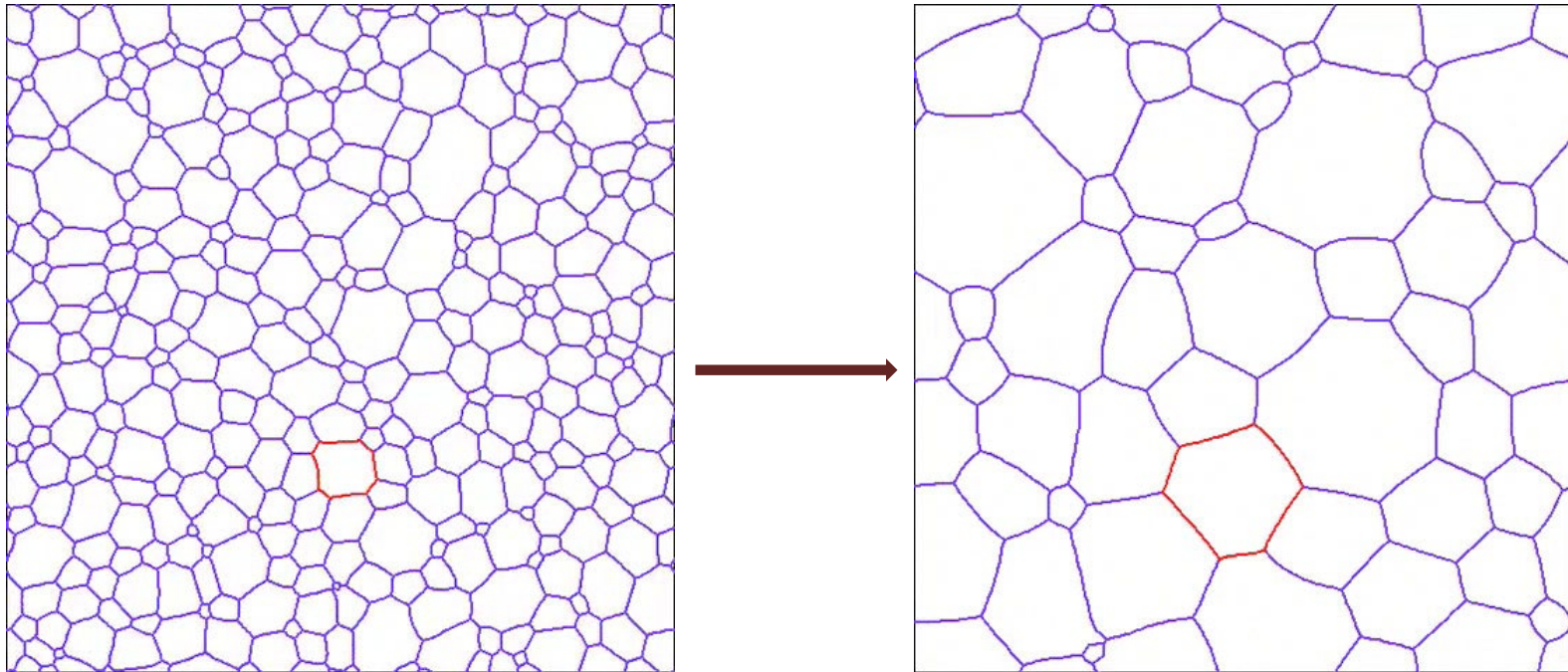


*J. J. Thomson, Proc. Cambridge Philos. Soc. **11**, 120 (1901).*

*Barmak et al. J. Appl. Phys. **120**, 065106 (2016).*

# Engineering the Grain Structure

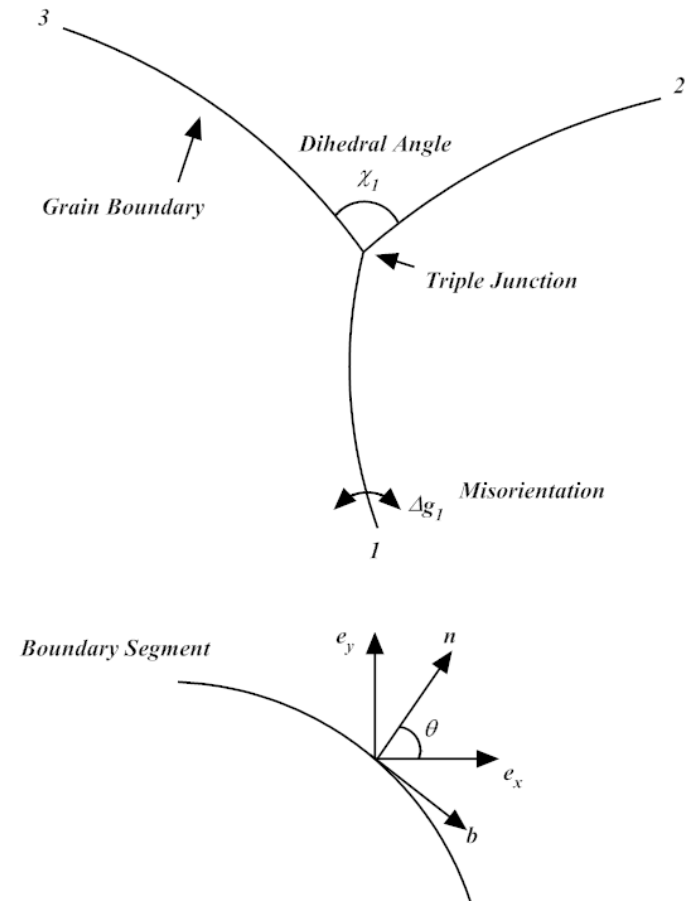
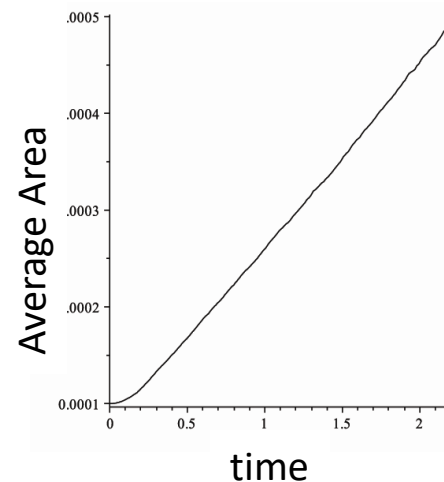
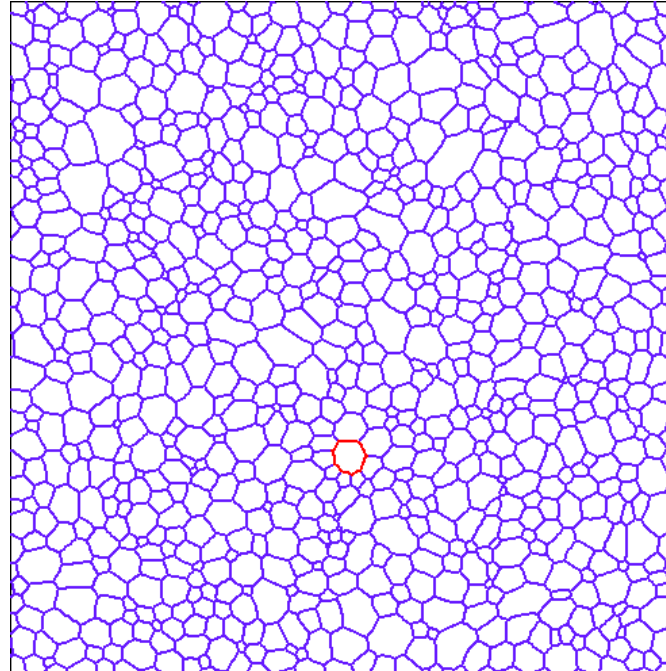
One method by which the grain structure is engineered is through **grain growth** or coarsening of a starting structure.



- Grain boundaries are “defects”; in pure materials they represent regions of higher energy
- Grain boundaries are not equilibrium defects; thus, upon annealing, the structure evolves so as to reduce the total boundary energy

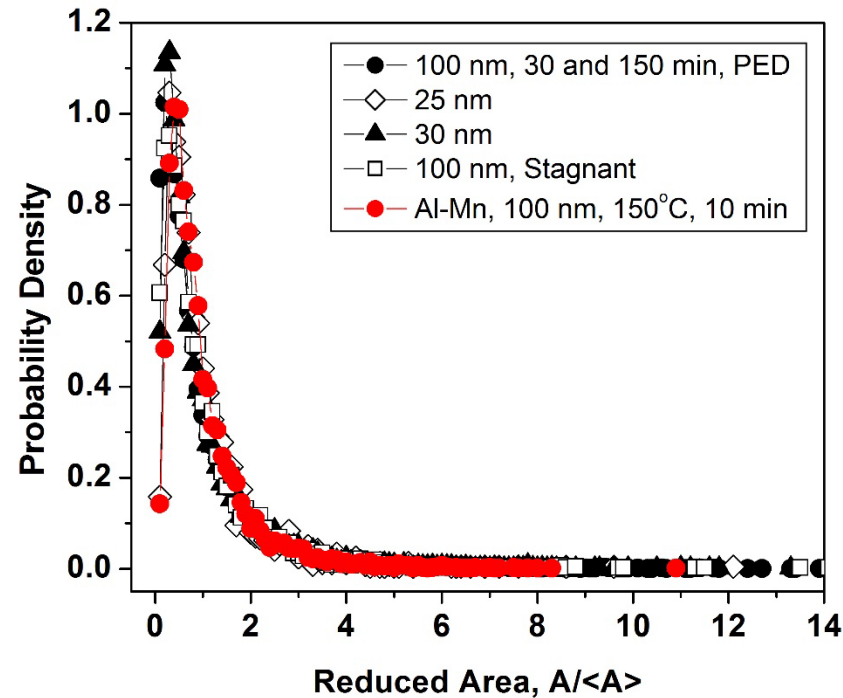
# Grain Growth Simulations in 2D

- Sharp interface simulation of curvature-driven coarsening, with isotropic boundary energy and mobility
- Boundary condition at triple junctions – Herring condition of normal and tangential force balance
- Grains follow the von Neumann-Mullins ( $n-6$ ) rule in the period between critical events (or topological discontinuities)

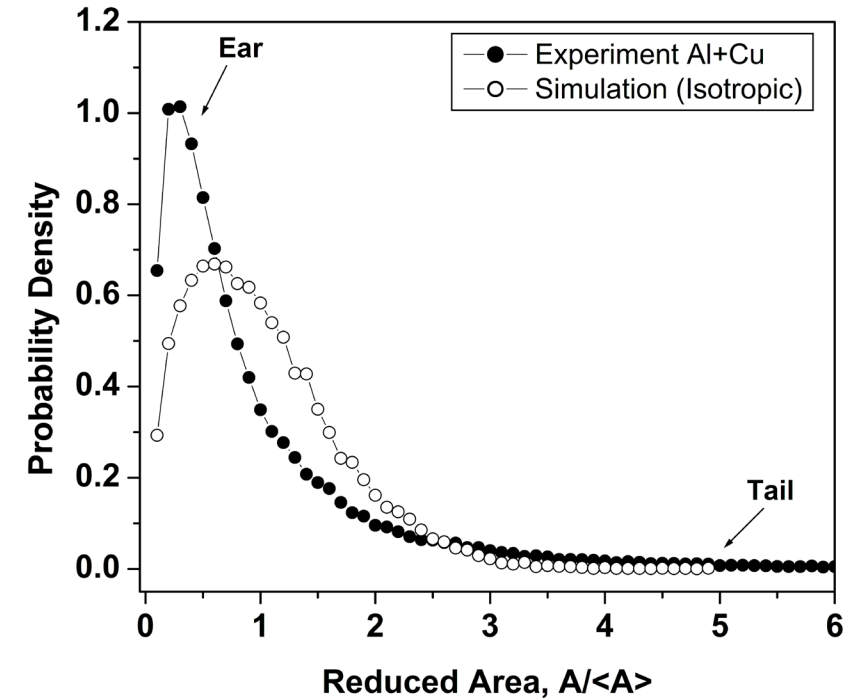


*C. Herring, The Physics of Powder Metallurgy, ed. W. E. Kingston, McGraw-Hill Book Co., New York (1951) p. 143.*

# Grain Size Distribution: Thin Film Experiments



Experimental grain size data from thin Al and Al-0.2at%Mn films collected over a 25-year period by using both semi-automated and automated image analysis and crystal orientation mapping methods.

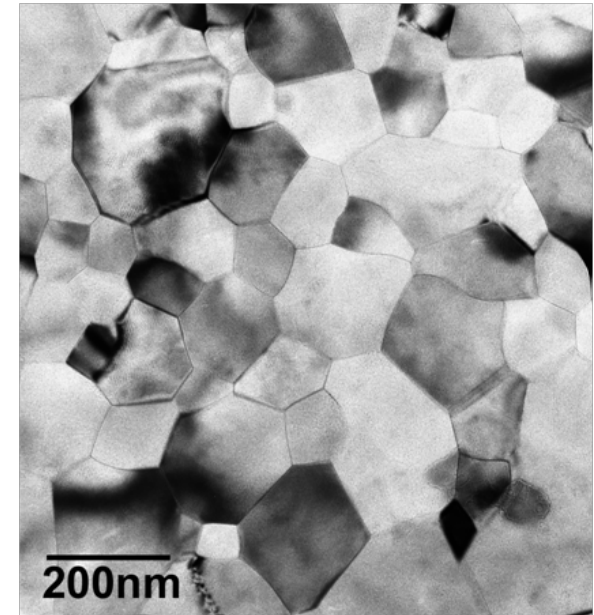


“Universal” experimental grain size distribution (of 58,346 grains) for Al and Cu films is compared with results for sharp-interface grain growth simulations with isotropic grain boundary energy.

# Grain Growth: Metrics of Grain Structure

- Geometric
  - Size
  - Dihedral angle distribution
  - Convex hull ratio
- Topological
  - Sides
  - Average side class of neighbors
- Geometrical-Topological
  - Size-sides

Historically, the focus of nearly all experiments and simulations.

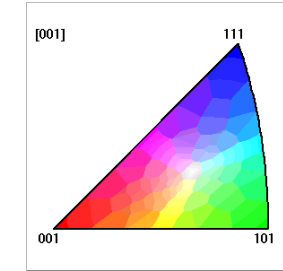
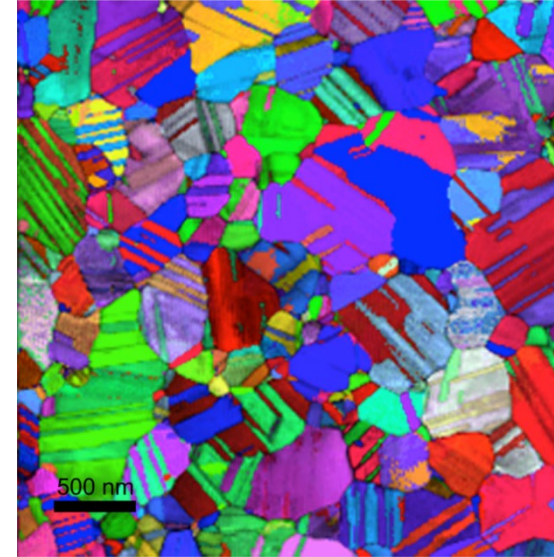
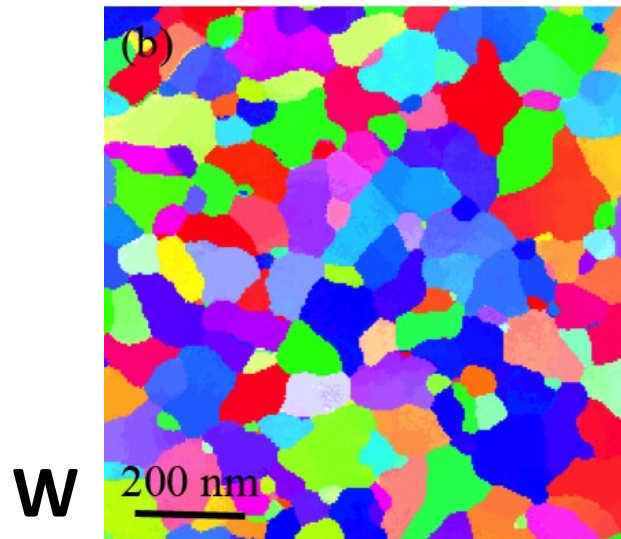
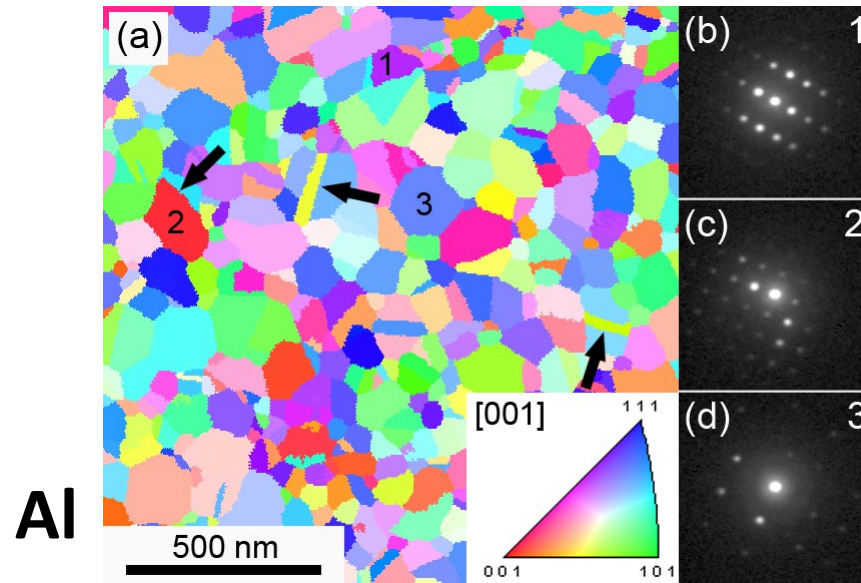


Aluminum

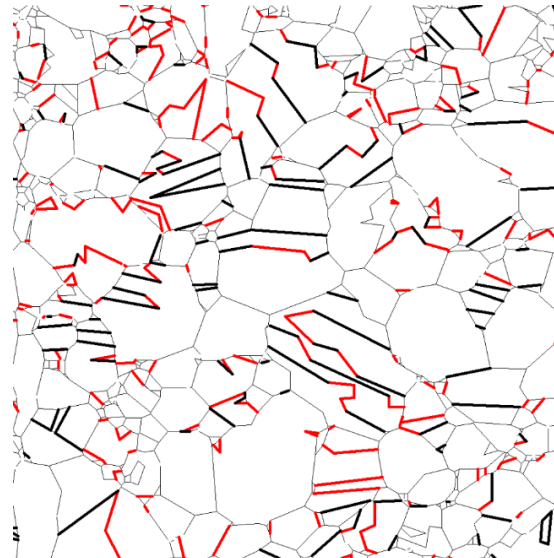
*K. Barmak, E. Eggeling, D. Kinderlehrer, R. Sharp, S. Ta'asan, A. D. Rollett, K. R. Coffey,  
"Grain Growth and the Puzzle of its Stagnation in Thin Films: The Curious Tale of a Tail and an Ear",  
Progress in Mater. Sci. 58, 987-1055 (2013).*



# Orientation Mapping Using Precession Electron Diffraction in the TEM



**Cu**



**Thick black lines:**  
coherent twin boundaries

**Thick red lines:**  
incoherent twin boundaries

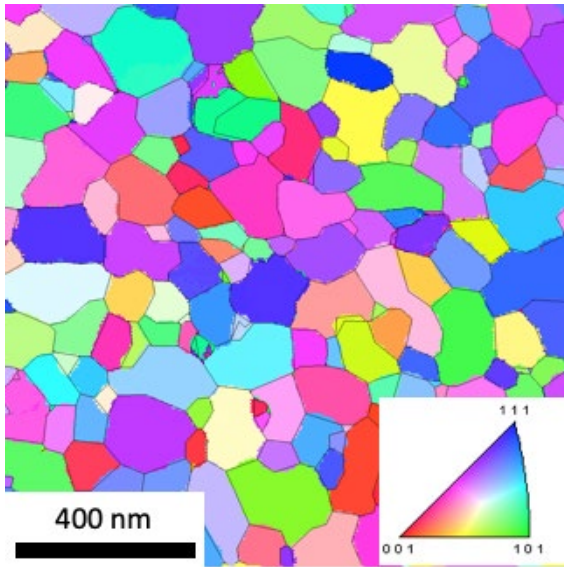
# Metrics of Grain Structure

---

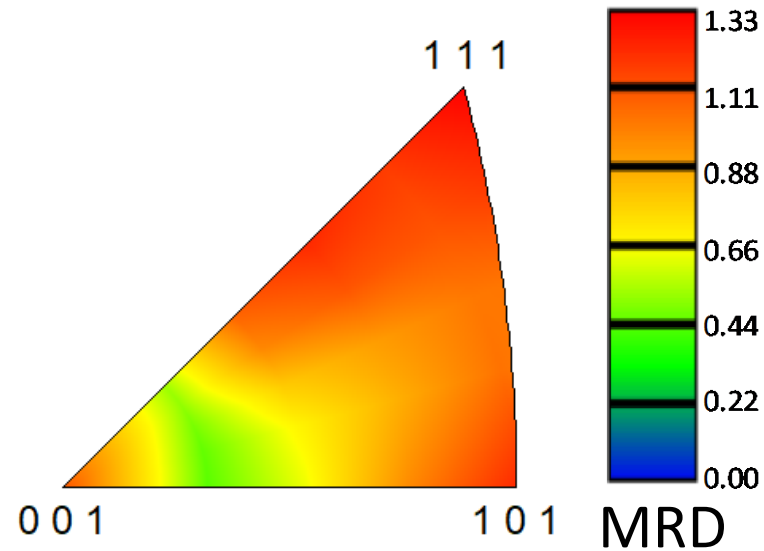
- Energetic
  - Grain boundary character distribution (GBCD)
  - Grain boundary energy distribution (GBED)
- Dynamic
  - Motion of grain boundaries and triple junctions
  - Pinning of boundaries and triple junctions
  - Rates of critical events
- Correlations
  - Spatial, crystallographic, temporal

# Tungsten: W

Disorientation distribution  
and pair correlation function

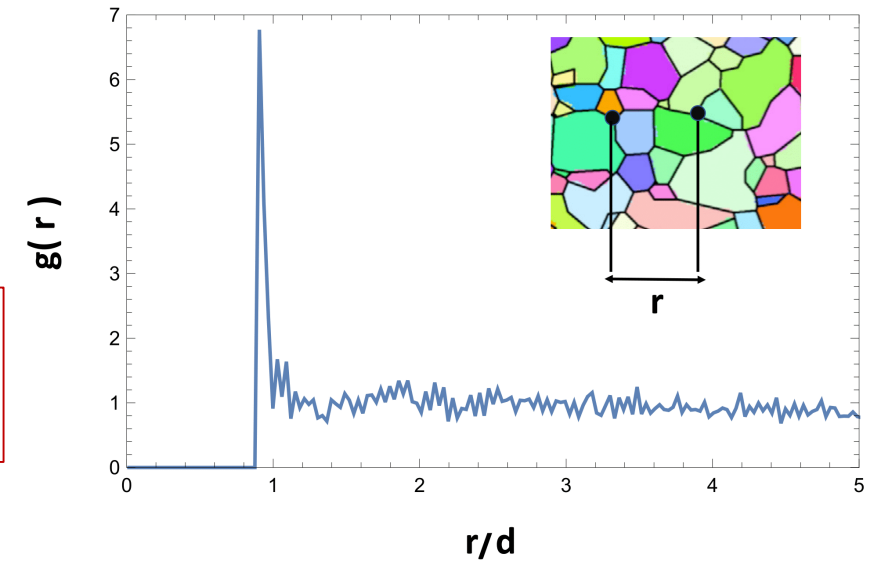
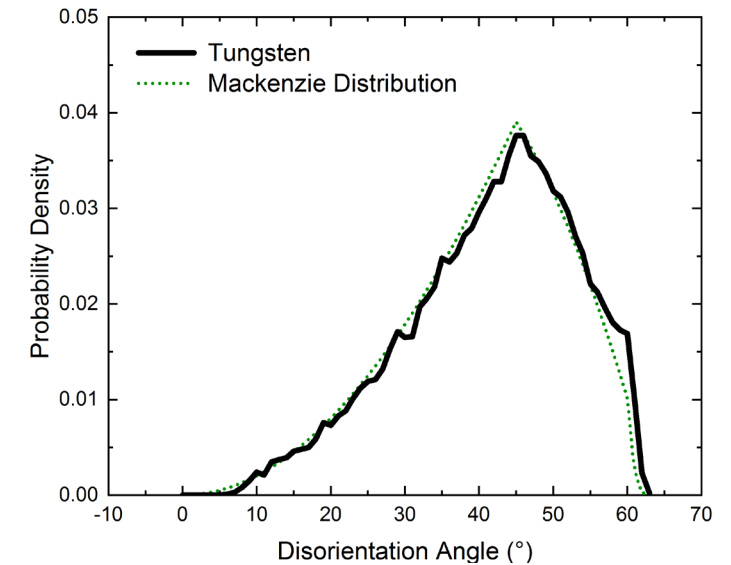


Inverse pole figure map in  
sample normal direction



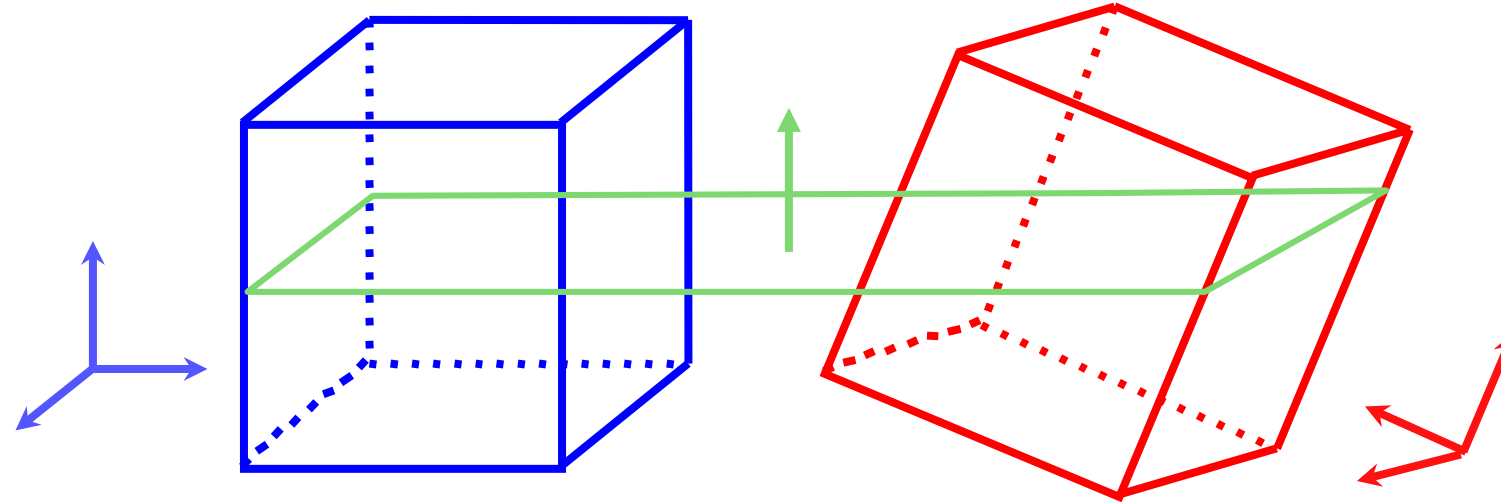
Orientation distribution  
for one field of view

Nominally 40 nm-thick tungsten film  
Deposited at room temperature, annealed 2h at 850°C



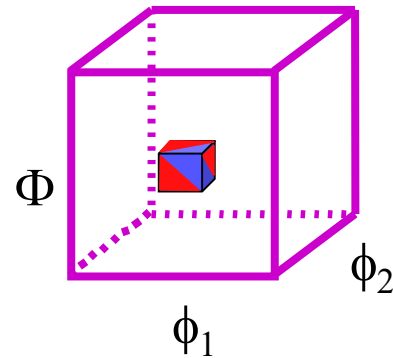
# Grain Boundary Character Distribution: Relative Area(Length) in 3D(2D)

Grain size in the nanometer to micrometer range

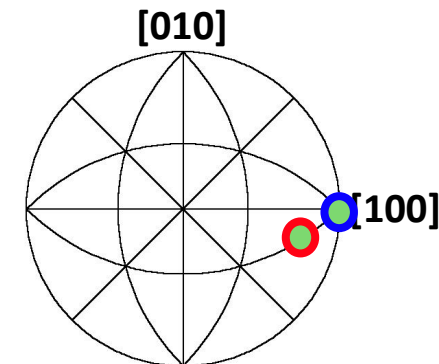


Lattice Misorientation

Boundary Plane



Three Euler angles



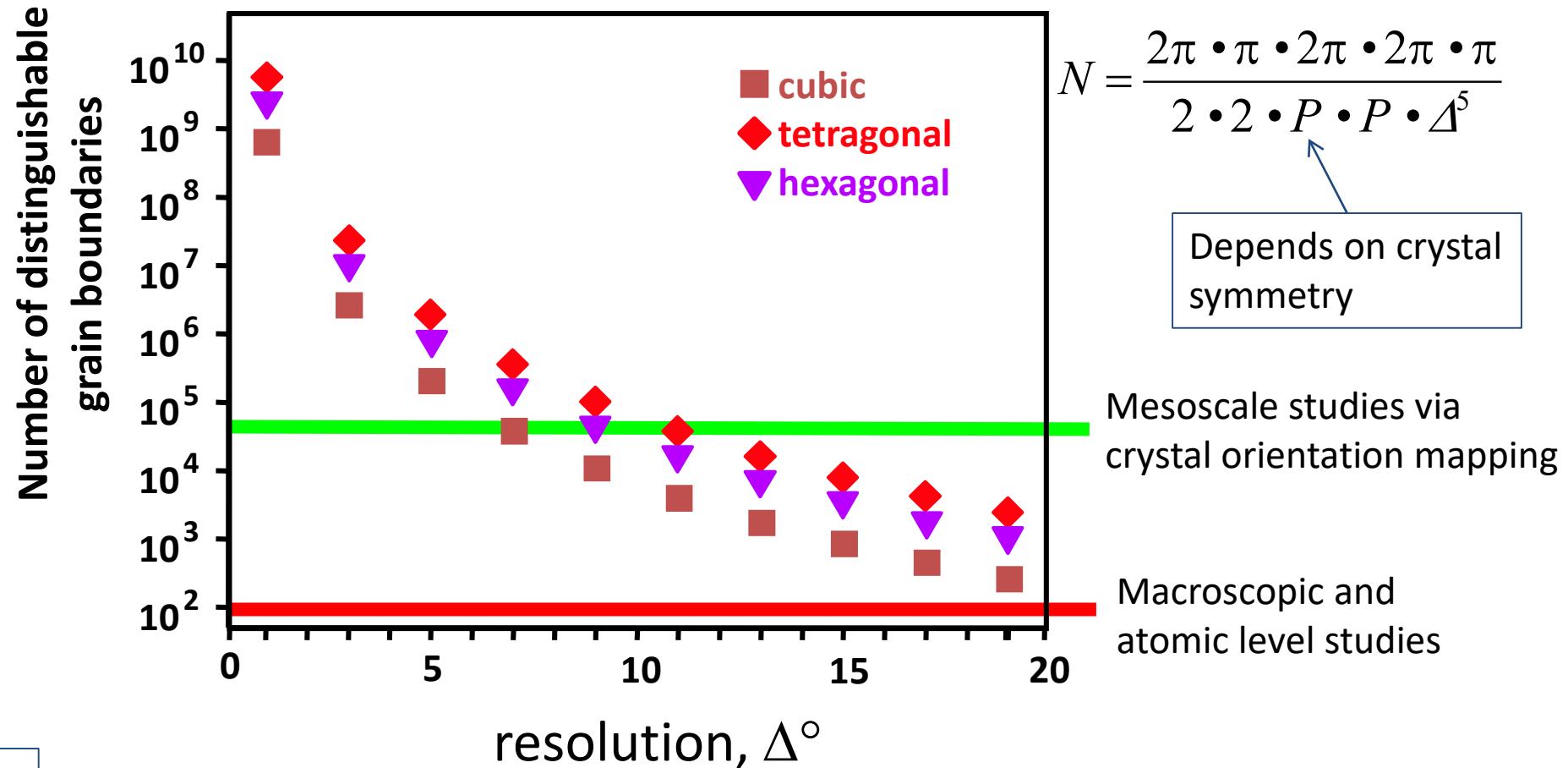
Two spherical angles

G. S. Rohrer

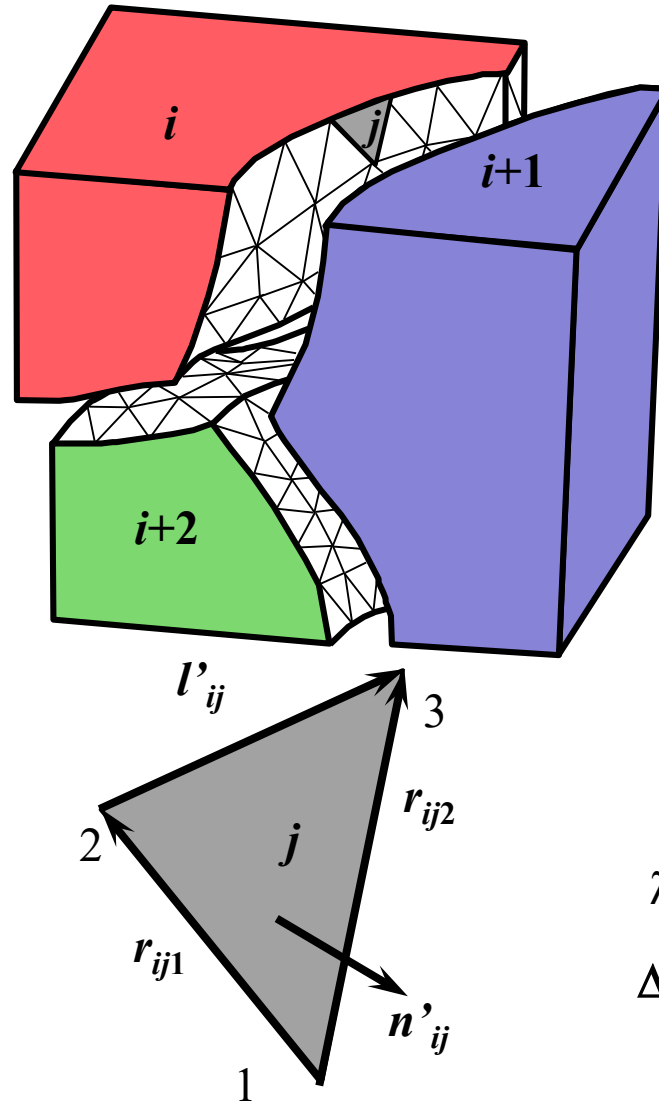
There are five macroscopically observable grain boundary parameters



# GBCD: Classification of Grain Boundaries



# GBCD: Relative Area(Length) in 3D(2D)



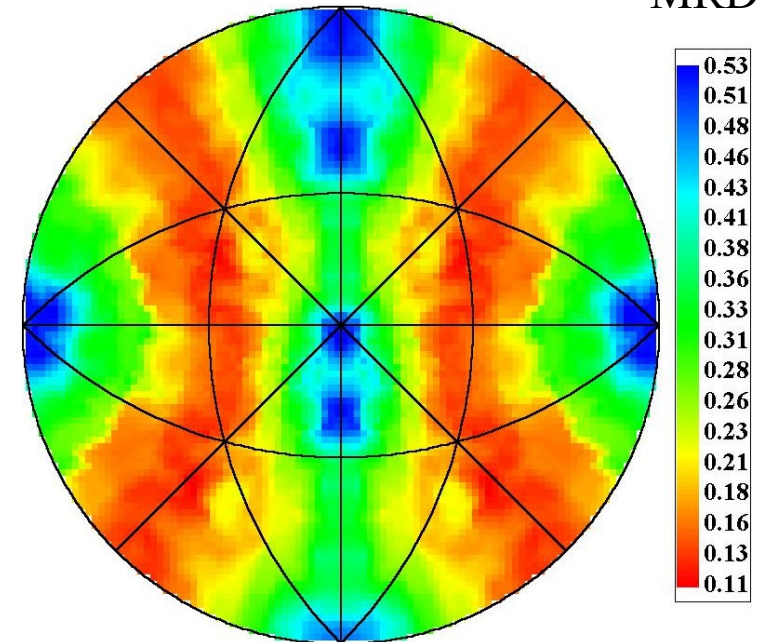
Index  $n'$  in the **bicrystal** reference frame, with respect to grains  $i$  and  $i+1$ .  
At  $\Delta g$ ,  $n = g_i n'$  and  $n = g_{i+1} n'$   
(5 parameter description)

$$\lambda(\Delta g, n)$$



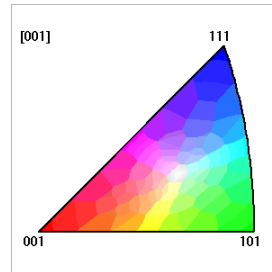
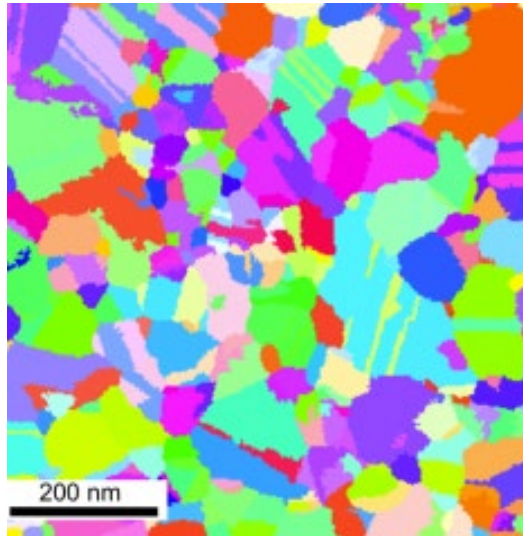
$$\lambda(n|\Delta g)$$

$$\Delta g = 35^\circ/[100]$$

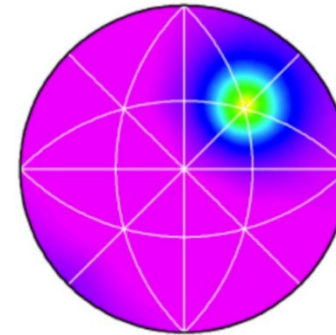


MRD

# Grain Boundary Character Distribution: Cu and Al



## Copper

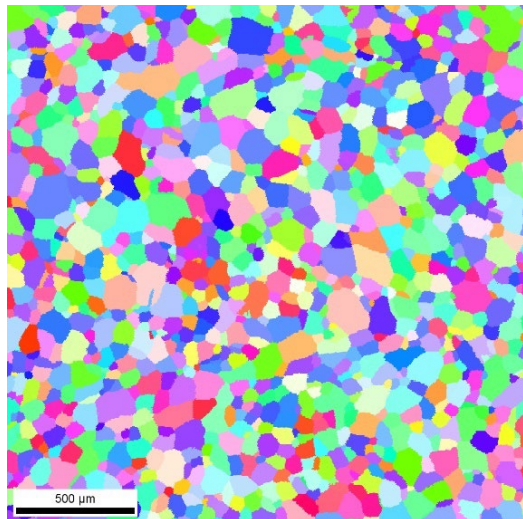


Misorientation

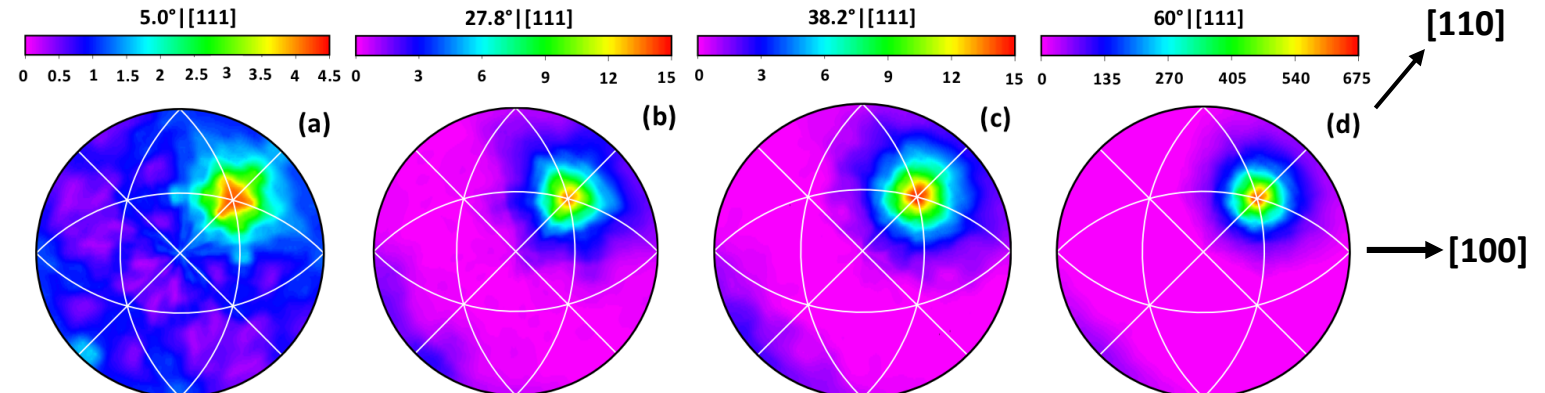
$\lambda(60^\circ/[111])$ , MRD

MRD = Multiples of random distribution

0 100 200 300 400 500 600 700 800 900  
Multiples of Random

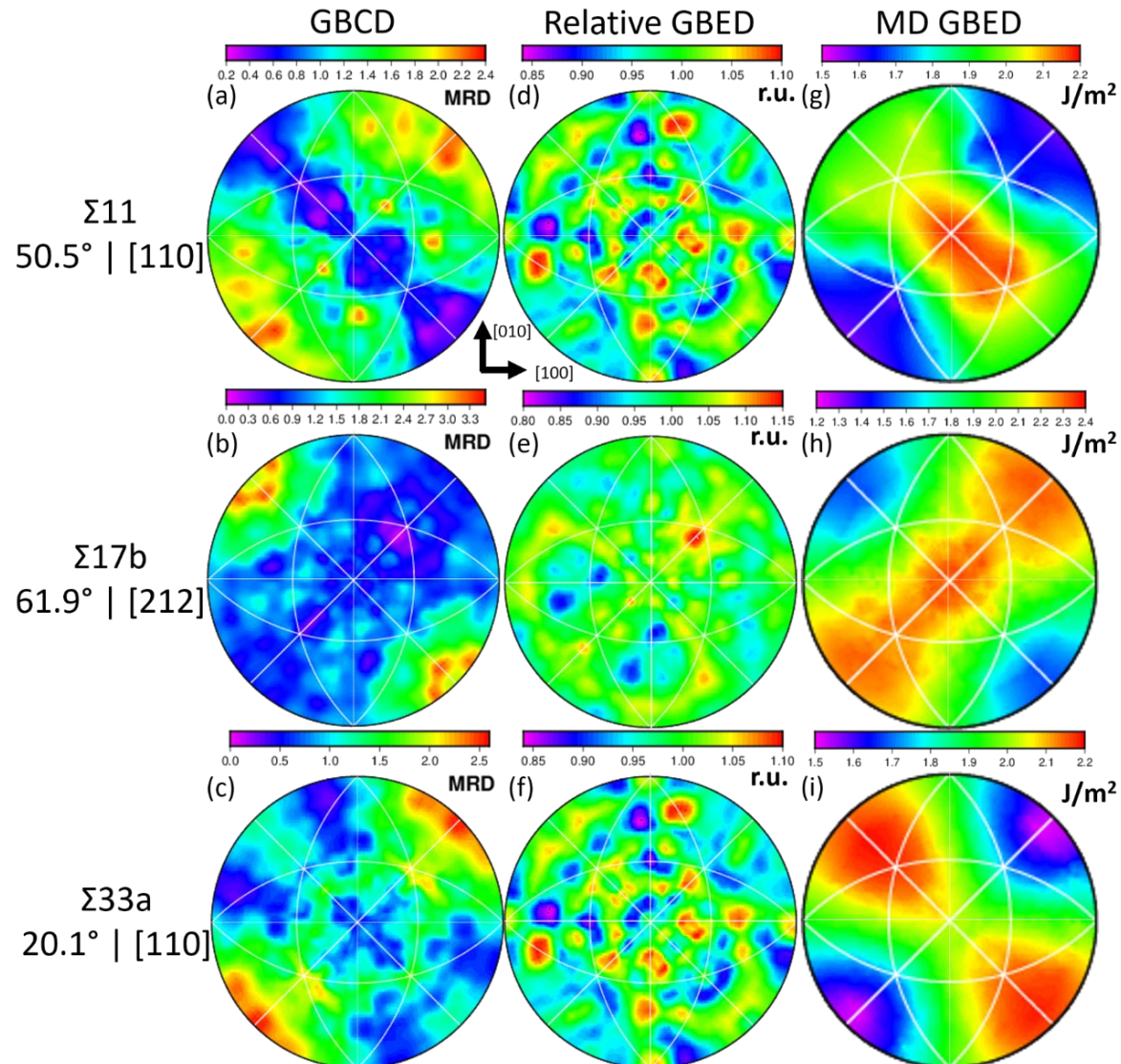


## Aluminum

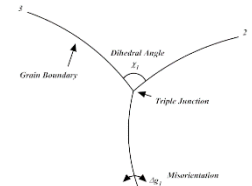




# W: GBED, Relative and MD-Computed GBED

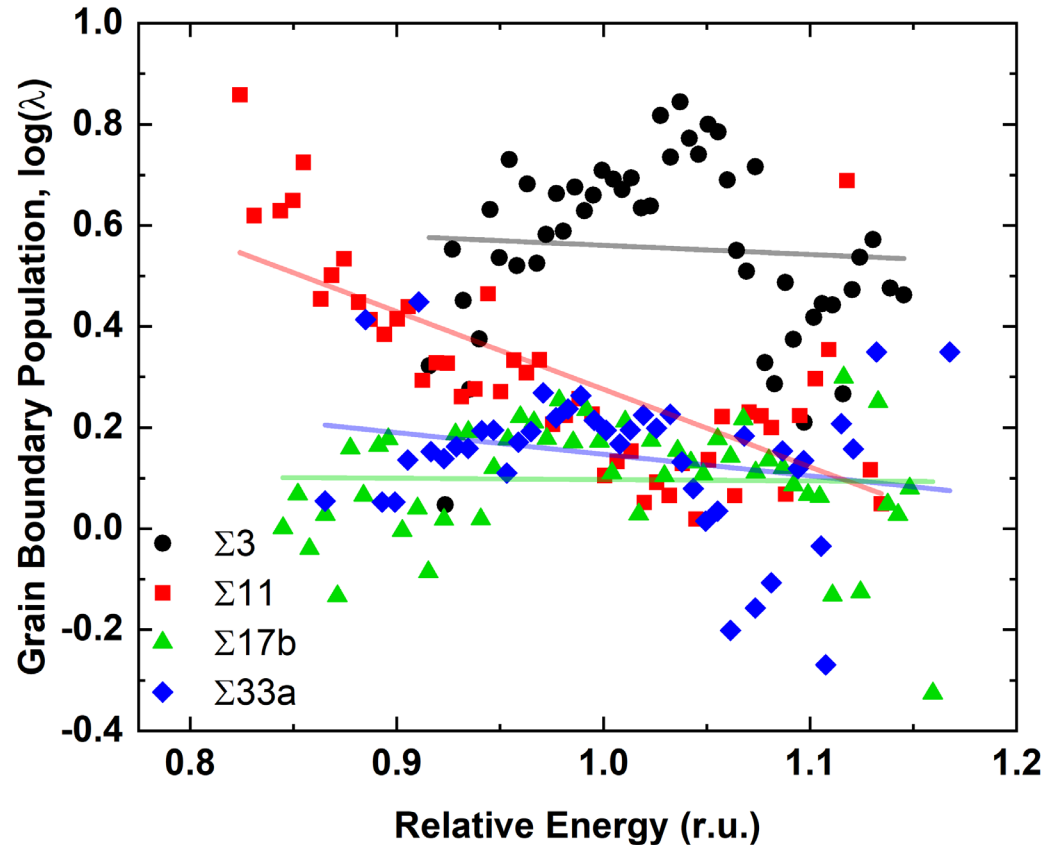


- GBED for this W film correlates well with GBED for microcrystalline, bcc steel
- GBED and MD-computed energies are inversely correlated, as in microcrystalline materials
- Relative GBED extracted from triple junction geometry under the assumption of Herring equilibrium neither correlates with MD GBED nor inversely with GBED

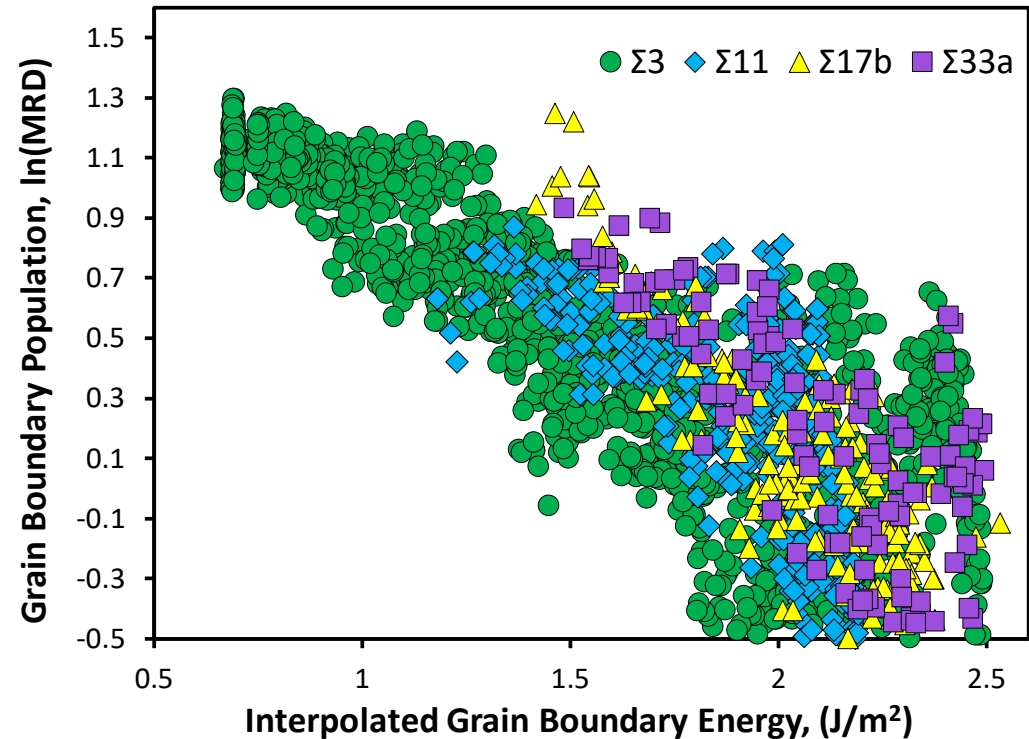




# W: Population, Relative and MD-Computed Energy



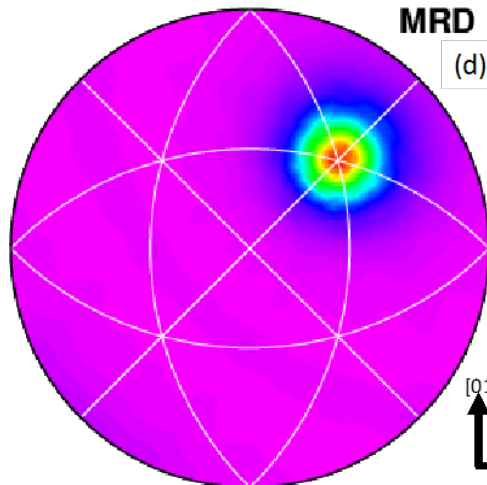
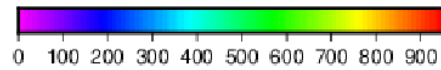
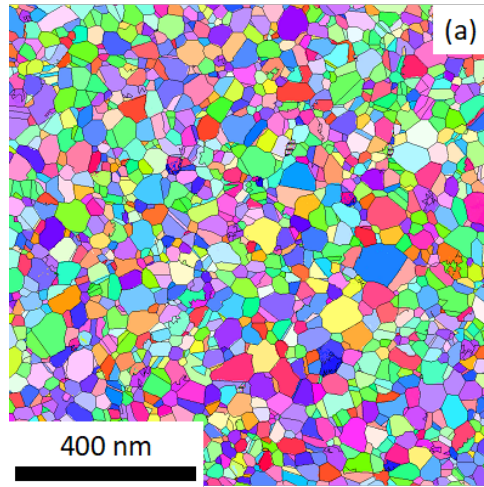
The inverse correlation with relative energies is not observed



The surprise here is that grain boundary populations vs. MD-computed and interpolated energies are so well-behaved despite the fact that there was no grain growth in the W films.

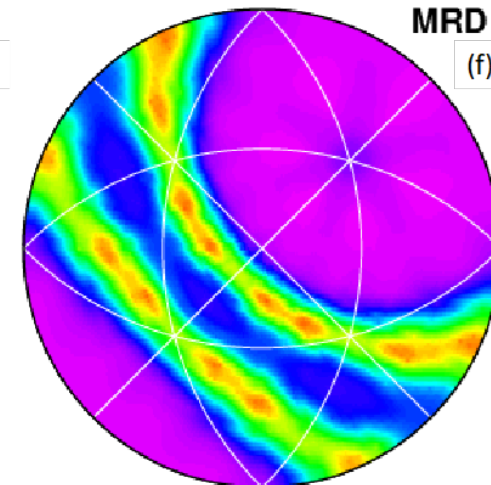
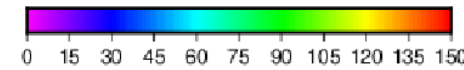
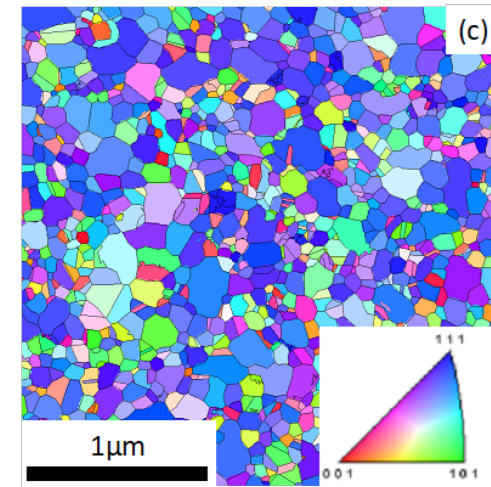
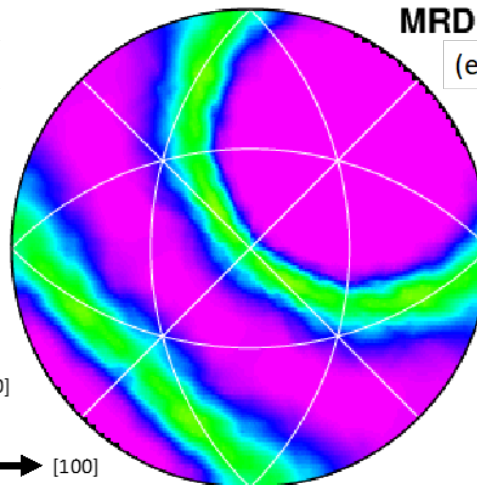
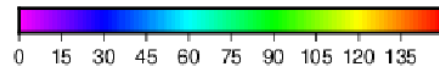
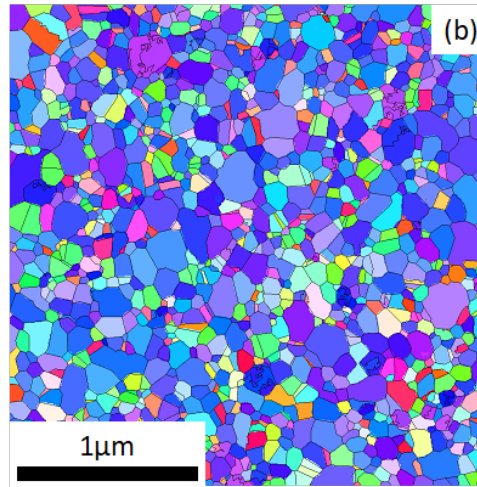
# Al: GBCD

As-deposited



$\lambda(60^\circ/[111])$

Twist



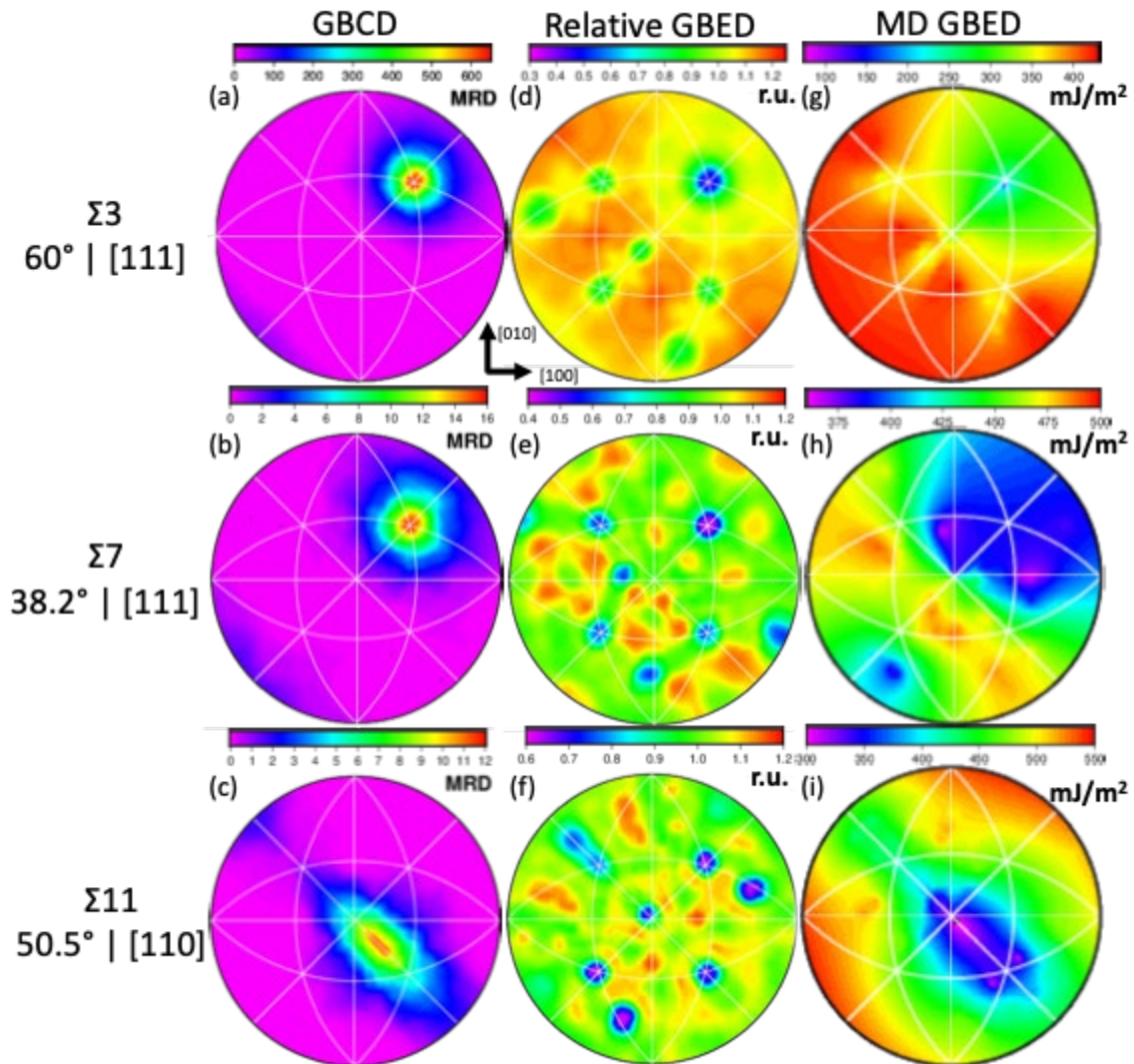
Increasing  
orientation texture

Annealed at 400°C  
(b) 30 min  
(c) 150 min

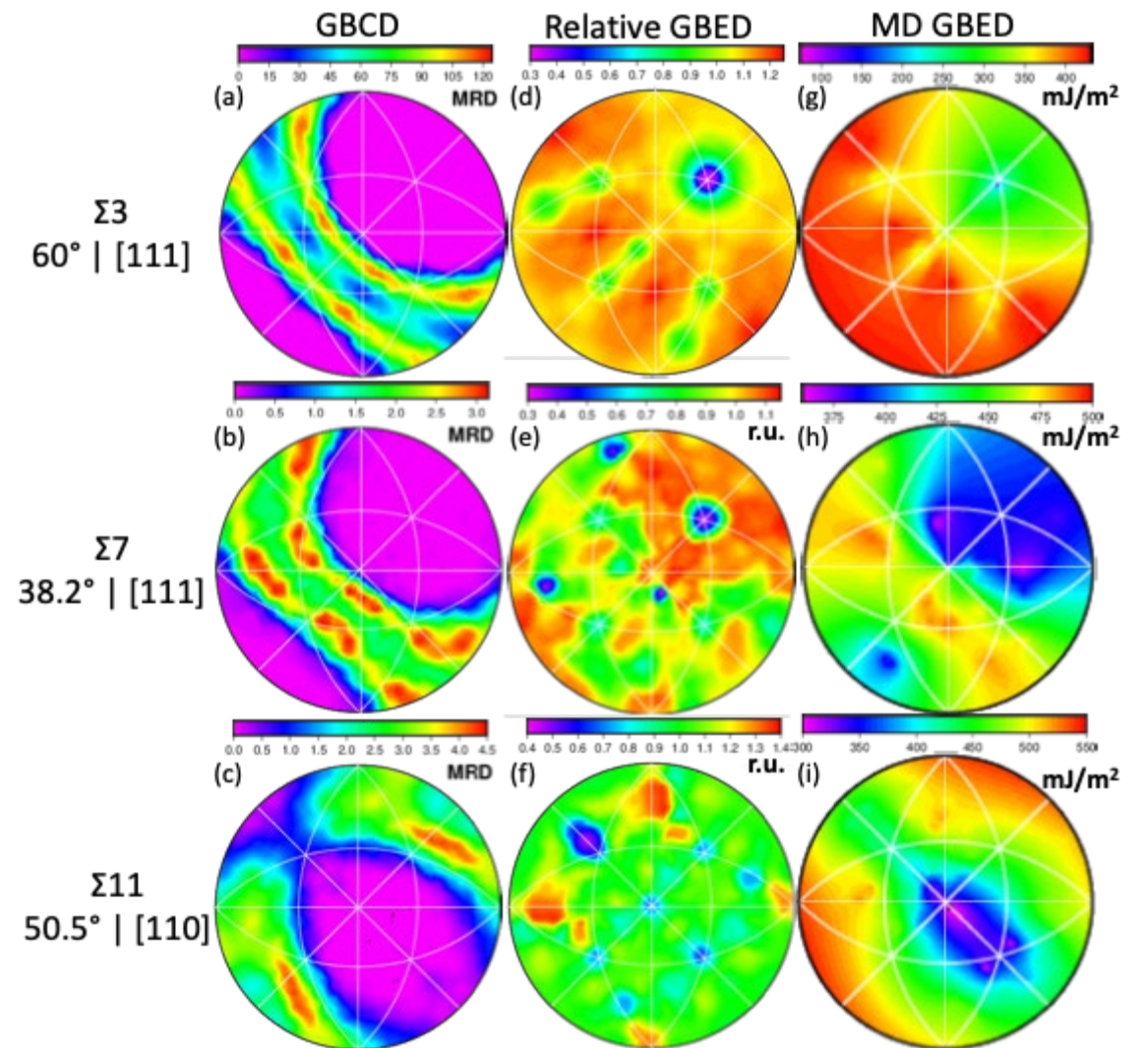
Tilt



# AI: GB~~CD~~-GB~~ED~~



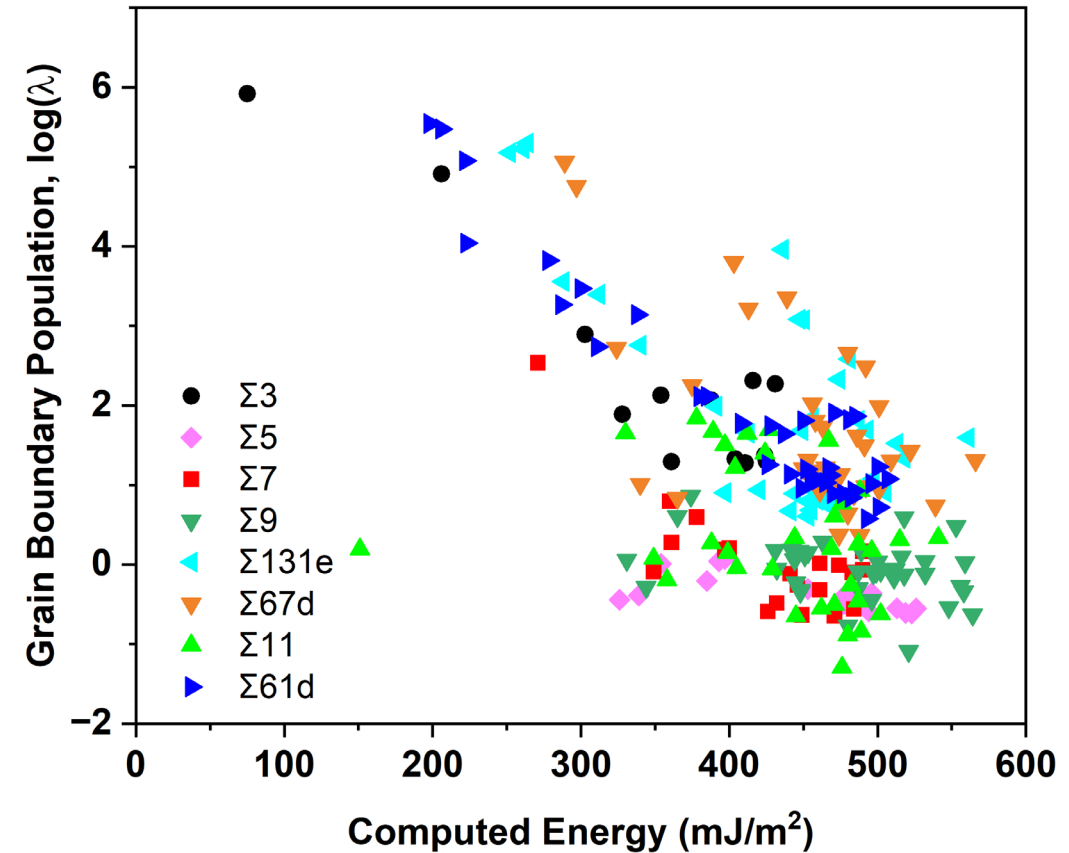
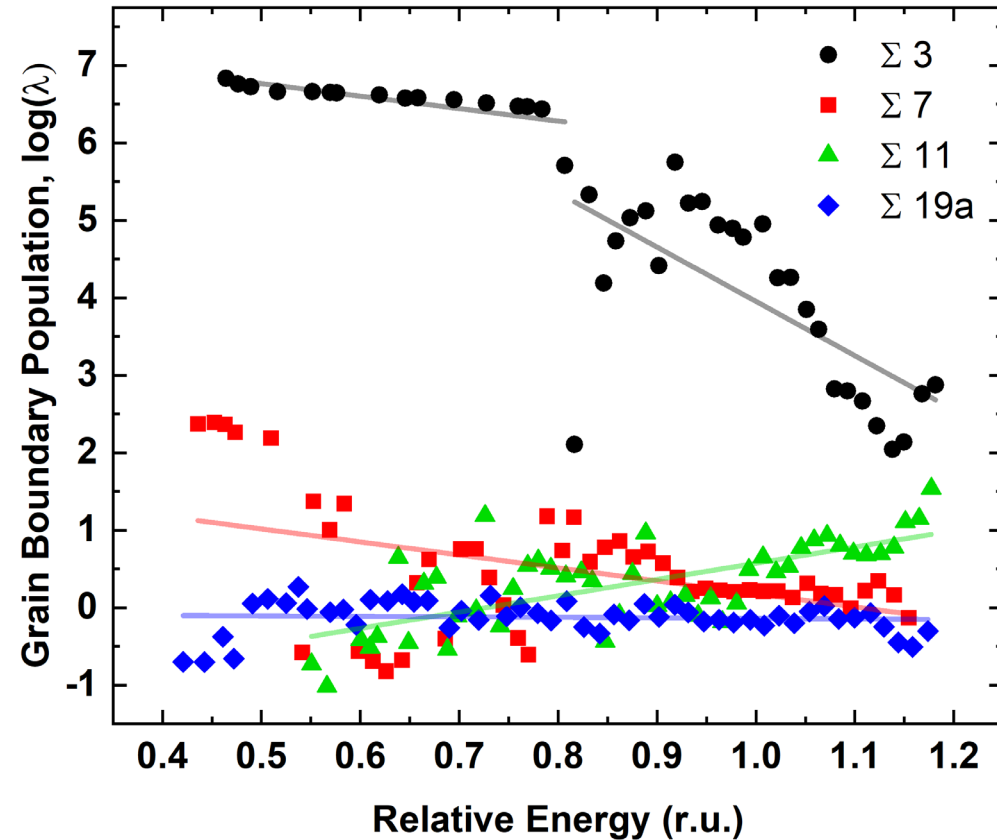
## As-Deposited



**400°C, 150 min**

# Al: Population, Relative and MD-Computed Energy

As-deposited



M. Patrick, G. Rohrer, O. Chirayutthanasak, S. Ratanaphan, E. Homer, G. W. Hart, Y. Epshteyn, K. Barmak, **Relative Grain Boundary Energies from Triple Junction Geometry: Limitations to Assuming the Herring Condition in Nanocrystalline Thin Films**, arXiv 2207.02313 .

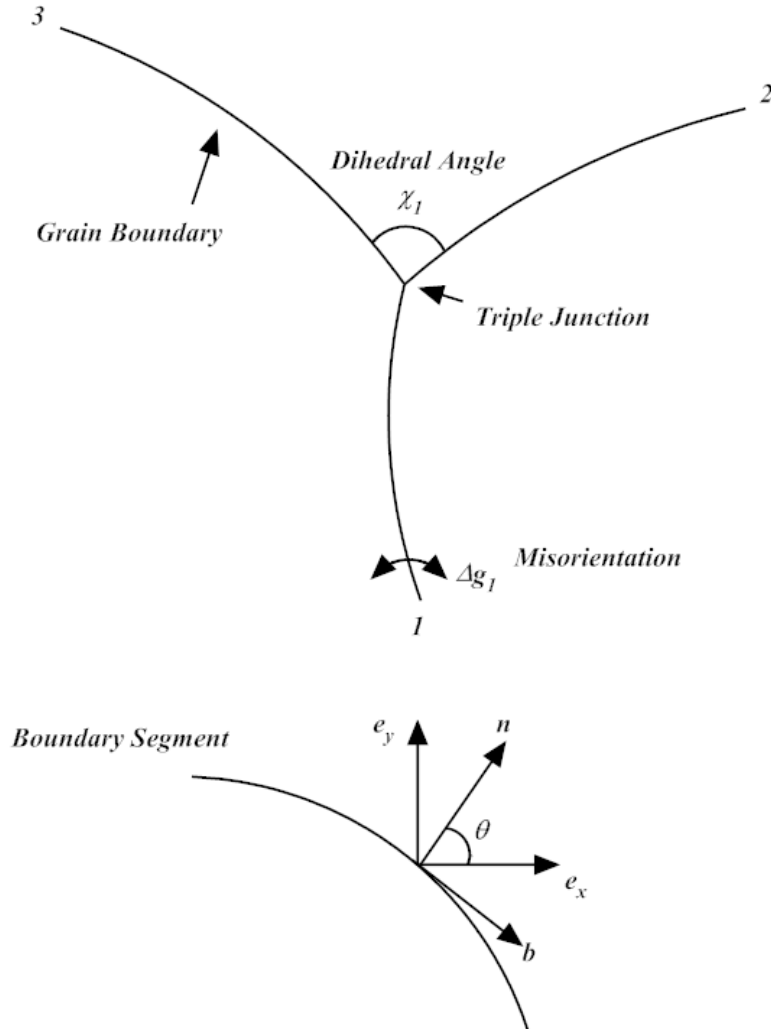


# Summary

---

- GBCD follows thermodynamic expectations
- However, the force equilibrium defined by the Herring equation cannot be used to extract relative energies in these films, and thus does not fully prescribe the triple junction geometry in these systems
- Therefore, other driving forces must also play a role in determining the behavior of the grain boundary network
- The results highlight the importance of triple junction behavior in the microstructure of polycrystalline materials

# Theory for GBCD – I



- Grain boundaries are smooth curves that meet at triple junctions or at the outside border of the configuration
- Boundary motion is curvature driven

$$\frac{d}{dt} E(t) = \sum_{k=1}^K \int_0^1 T^k \cdot \frac{dv^k}{ds} ds$$

$$T^k = \frac{\partial \sigma^k}{\partial \theta} n^k + \sigma^k b^k$$

Capillarity stress vector

# Theory for GB CD – II

- The Herring condition of normal and tangential force balance is enforced at triple junctions
- The evolution of the grain boundary network is dissipative and the maximum rate of boundary energy reduction in the interval between critical events occurs when boundaries move in the direction of their normals

$$\frac{d}{dt} E(t) = - \sum_{k=1}^K \int_0^1 \frac{1}{\mu^k} |v_n^k|^2 ds \leq 0$$

$$v_n^k = \mu^k \left( \frac{d^2 \sigma^k}{d\theta^2} + \sigma^k \right) K^k$$

In the absence of torque terms

$$v_n^k = \mu^k \sigma^k K^k$$

*C. Herring, The Physics of Powder Metallurgy. ed. W. E. Kingston, (McGraw-Hill Book Co., New York 1951) p. 143.*

# Theory for GB CD – III

---

- For anisotropic grain boundary energy, where energy is only a function of misorientation and not the boundary normal, we have:

$$\sigma = \sigma(\alpha)$$

- Define the GB CD,  $\rho(\alpha, t)$ , as relative length in 2D of arcs of grain boundaries sorted by the misorientation angle  $\alpha$  at time  $t$ , normalized such that

$$\int \rho d\alpha = 1$$

*K. Barmak, E. Eggeling, M. Emelianenko, Y. Ephshteyn, D. Kinderlehrer, R. Sharp, S. Ta'asan, Phys. Rev. B 83, 134117: (2011).  
P. Bardsley, K. Barmak, E. Eggeling, Y. Ephshteyn, D. Kinderlehrer, S. Ta'asan, Rend. Lincei Mat. Appl. 28, 777 (2017).*



# Towards a Gradient Flow for Microstructure – I

---

- **Critical events** of boundary or grain disappearance **introduce irreversibility** into the system
- To account for this irreversibility, an **entropic term is added** in the form of configurational entropy

$$F(\rho) = \int_{\Omega} (\sigma \rho + \lambda \rho \log \rho) d\alpha \quad \boxed{\text{Free energy}}$$

- Solved iteratively – Iterates of implicit scheme based on the variational principle known to give solution of Fokker-Plank Equation (Jordan-Kinderlehrer-Otto)

# Towards a Gradient Flow for Microstructure – II

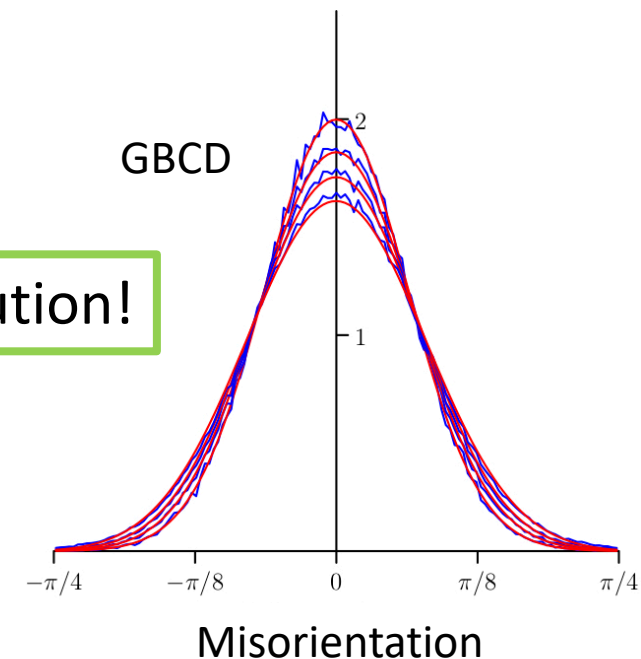
- Evolution of GBCD satisfies Fokker-Planck
  - A stationary distribution is obtained

$$\rho_\lambda \rightarrow \frac{1}{Z_\lambda} e^{-\frac{\sigma}{\lambda}} \quad \text{as } t \rightarrow \infty$$

$$Z_\lambda = \int_{\Omega} e^{-\frac{\sigma}{\lambda}} d\alpha$$

Boltzmann Distribution!

Empirical GBCD from **2D simulations**  
vs. **Fokker-Planck Solution**



Y. Epshteyn, C. Liu, M. Mizuno, *SIMA* **53**, 3072(2021).

K. Barmak, A. Dunca, Y. Epshteyn, C. Liu, M. Mizuno, *AWM-Springer Volume*, in press, *arXiv:2105.07255*, (2022).

Y. Epshteyn, C. Liu, M. Mizuno, *submitted*, *arXiv:2106.14249*, (2021).

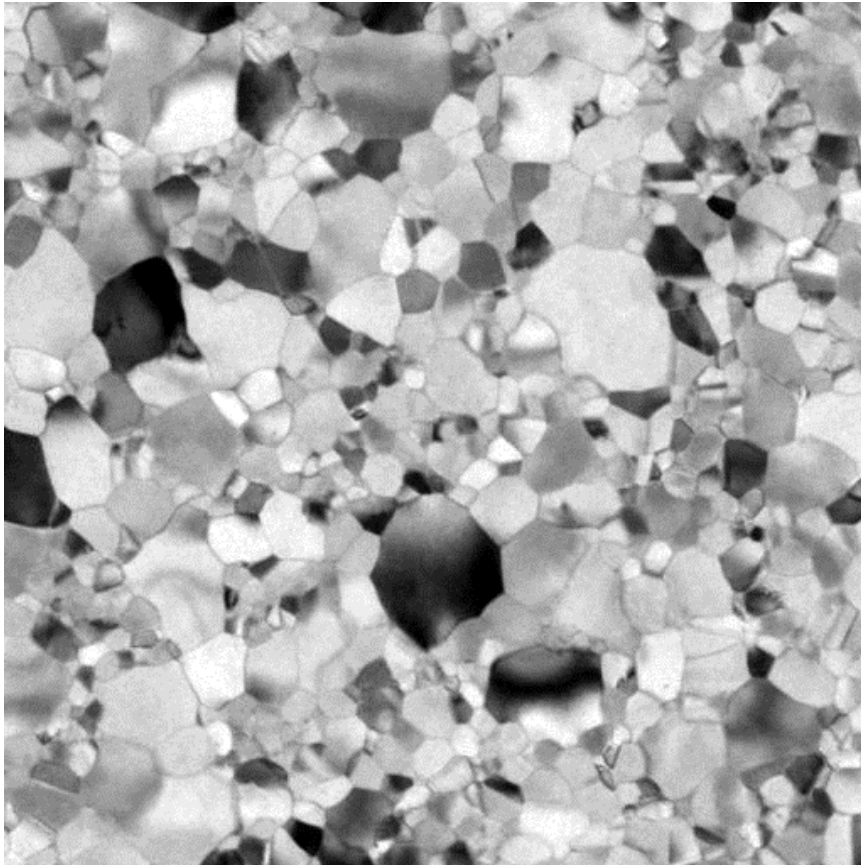
# Metrics of Grain Structure

---

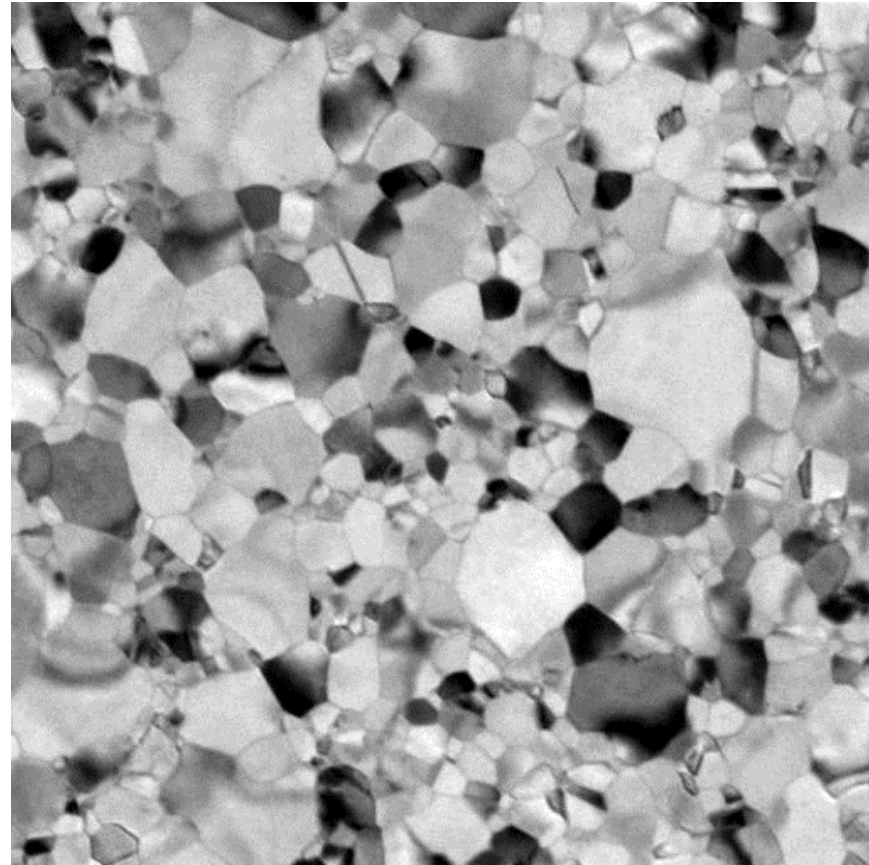
- Energetic
  - Grain boundary character distribution (GBCD)
  - Grain boundary energy distribution (GBED)
- Dynamic
  - Motion of grain boundaries and triple junctions
  - Pinning of boundaries and triple junctions
  - Rates of critical events
- Correlations
  - Spatial, crystallographic, temporal

# *In Situ* Grain Growth Studies: Pt

300-400°C



400-500°C

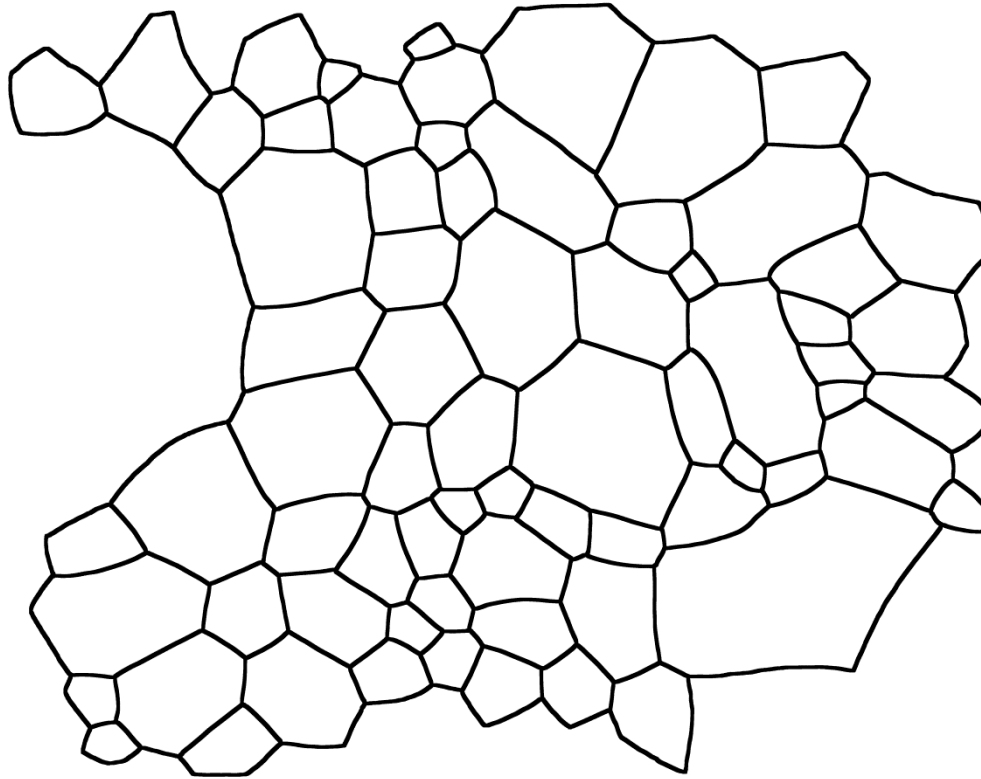




# Experiments: Imaging and Boundary Detection

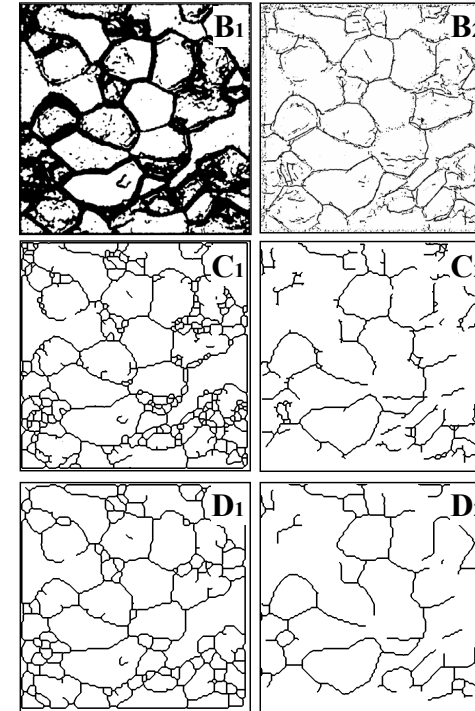
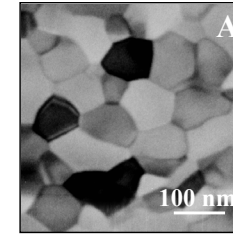
Aluminum

Manual tracing



Use 2-4 images at different sample tilts.

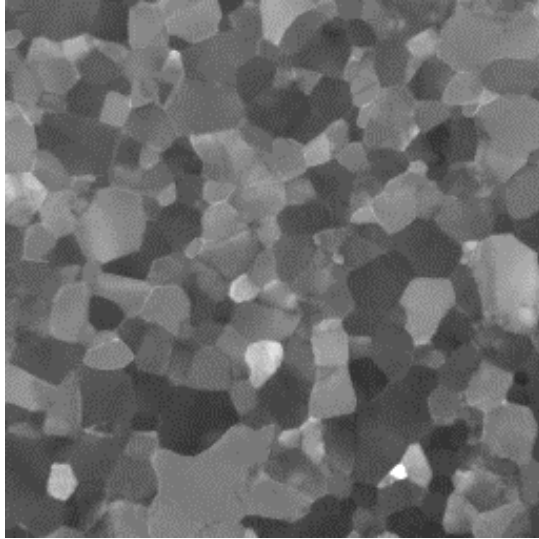
Automated



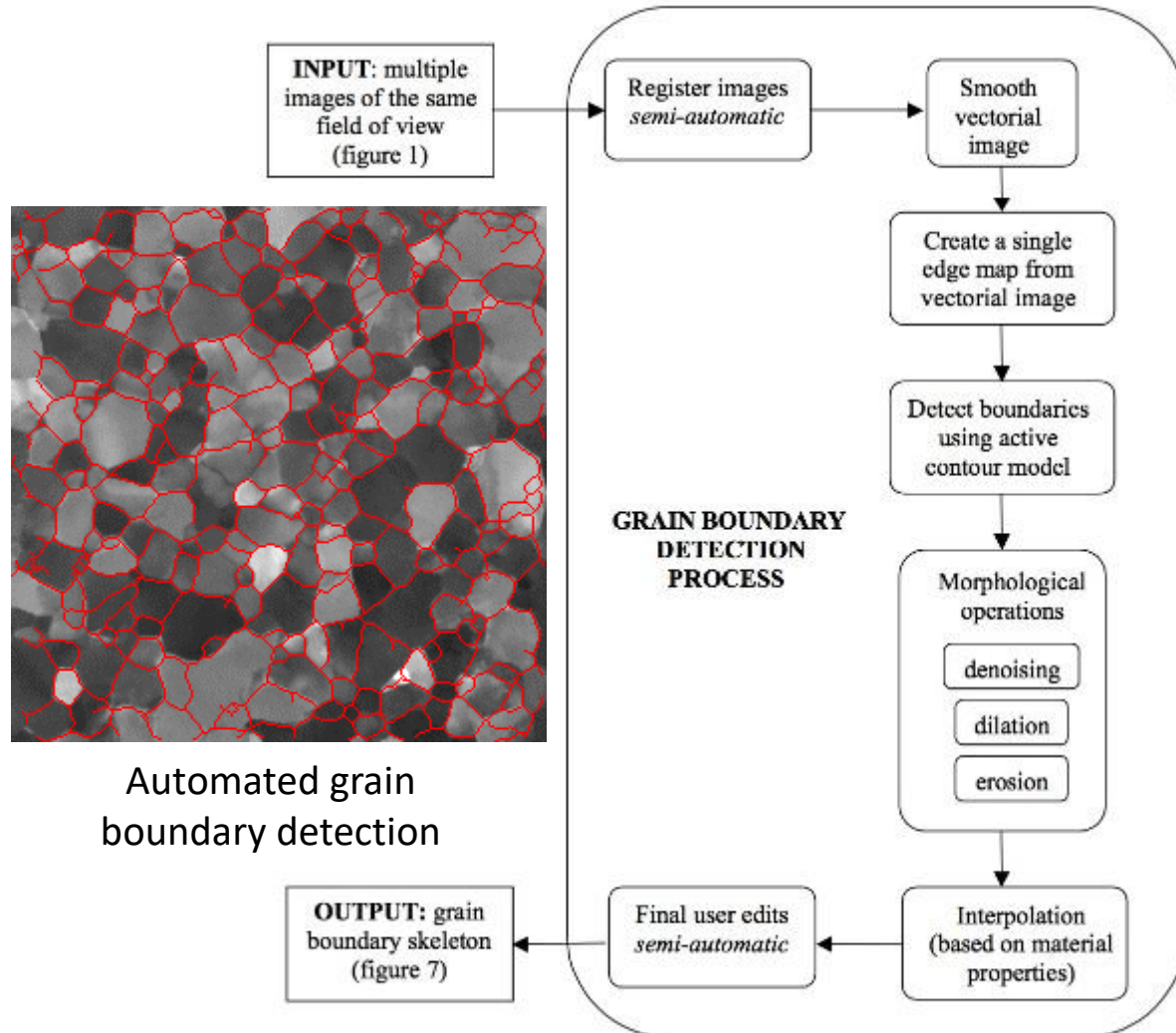
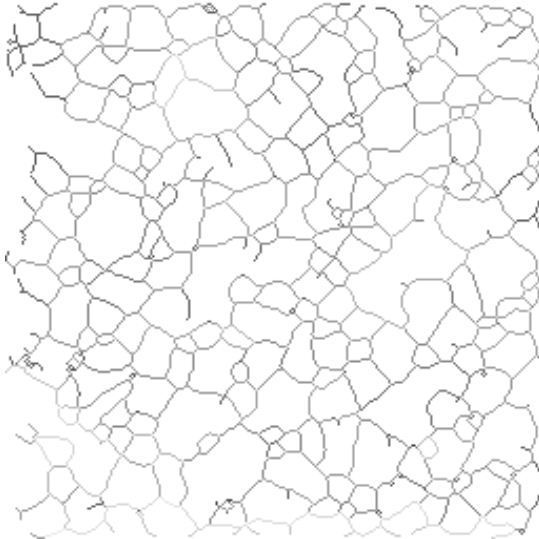
*D. T. Carpenter et al. J. Appl. Phys. 84, 5843 (1998).*

# Automated Grain Boundary Detection – I

Platinum

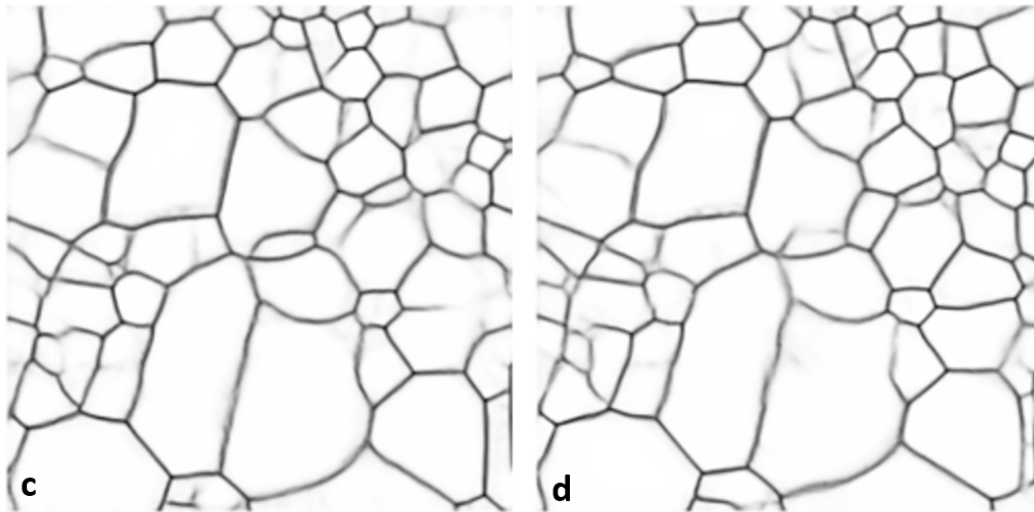
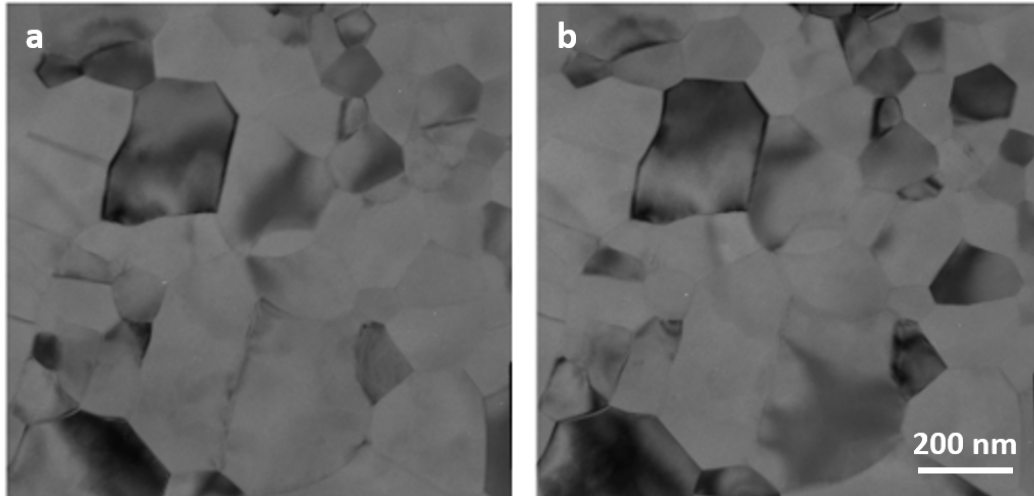


1 of 10 Pt images of the same FoV

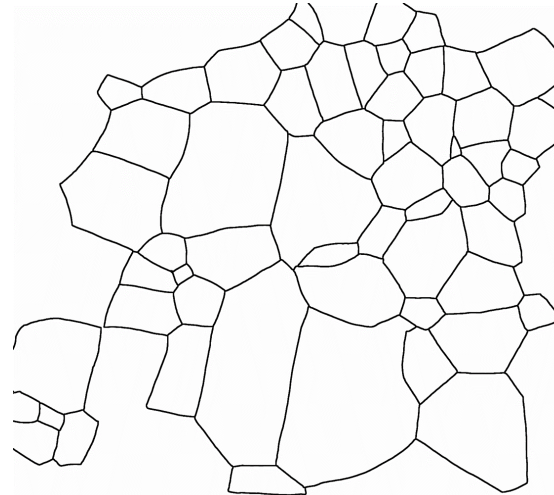


K. Barmak, P. Cancela, J. Esposito, D. Hower, S. Levine, G. Randall, (2007).

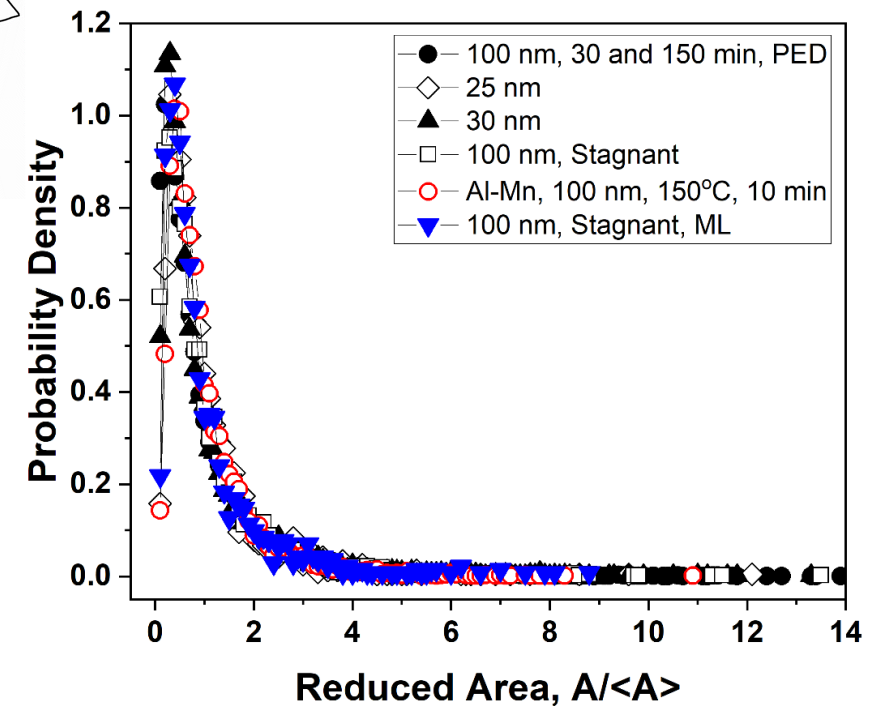
# Automated Grain Boundary Detection – II



ML-based boundary tracing



Manual tracing:  
“Ground truth”



# Summary and Conclusions

---

- For development of a predictive, prescriptive theory of grain growth:
  - ***In situ* experiments** are central to the determination of mechanisms of motion and pinning, as well the rates of critical events statistics that are required for development of grain growth models and theories
  - ***Ex situ* experiments** are key to the geometric, topological and energetic statistics needed for detailed comparison of simulations and experiments
  - **Close integration of experiments** (including automated image processing) and **simulations**, together with more advanced approaches to **data analytics**, are also critical to guiding **theory development**



# Acknowledge

kb2612@columbia.edu



**Katayun Barmak**  
Materials Science



**Yekaterina Epshteyn**  
Applied Mathematics



**Chun Liu**  
Applied Mathematics



**Jeffrey Rickman**  
Materials Science/Physics



Standing from left to right: M. Patrick (G), S. Toderas (UG), J. Lopez (UG), K. Barmak.  
Insets: J. Eckstein (UG), A. Ma (UG).

S. Levine (Duquesne Univ.)  
E. R. Homer, G. L. W. Hart (BYU)  
O. Chirayutthanasak, S. Ratanaphan (KMUTT, Thailand)  
G. S. Rohrer (CMU)